

Lrriq1 is an essential factor for fertility by suppressing apoptosis

Mayu Fukutomi¹, Chiharu Uedono¹, Aki Fujii¹, Youichi Sato^{1*}

¹ Department of Pharmaceutical Information Science, Tokushima University Graduate School of Biomedical Sciences, Tokushima, Japan

* Address correspondence to: Youichi Sato, Ph.D.

Department of Pharmaceutical Information Science, Tokushima University Graduate School of Biomedical Sciences

1-78-1 Sho-machi, Tokushima, Tokushima 770-8505, Japan

Phone: +81-88-633-7253; FAX: +81-88-633-7253

E-mail: youichi.sato@tokushima-u.ac.jp

Abstract

Purpose Leucine-rich repeats and IQ motif containing 1 (*LRRIQ1*) gene is reportedly associated with plasma inhibin B levels. However, the function of *LRRIQ1* remains unknown. In this study, we generated *Lrriq1* knockout mice (*Lrriq1*^{-/-} mice) and examined the effects of *LRRIQ1* on inhibin B and fertility.

Methods *Lrriq1*^{-/-} mice were generated using CRISPR/Cas9 genome editing technology. The expression of Inhibin B was examined by Western blotting using a protein extracted from the testis of a 3-month-old male mouse. Mating experiments were conducted using 7-week-old *Lrriq1*^{-/-} mice and wild-type (WT) mice to examine fertility. Sperm concentration and sperm motility were measured using 3-month-old male mice.

Results Expression analysis of inhibin B revealed that *Lrriq1*^{-/-} mice exhibited reduced mRNA and protein levels of inhibin alpha (*Inha*), which constitutes the α subunit. In the mating experiment, the litter size of *Lrriq1*^{-/-} male mice was 4.3 ± 2.9 , which was significantly lower than that of WT male mice (8.3 ± 1.3) ($p < 0.001$). No difference in sperm count was observed between *Lrriq1*^{-/-} and WT male mice; however, sperm motility (%) was significantly reduced in *Lrriq1*^{-/-} mice (48.4 ± 4.9) when compared with WT mice (70.2 ± 4.7) ($p < 0.001$). Based on TUNEL staining, the testes and epididymal sperm of *Lrriq1*^{-/-} mice showed high numbers of apoptosis-positive cells.

Conclusion *Lrriq1* knockout reduced sperm motility and litter size by inducing apoptosis of testicular germ cells and epididymal sperm.

Keywords: *Lrriq1*; Inhibin B; fertility; sperm motility; apoptosis

Introduction

Hormones are physiologically active substances synthesized and secreted by endocrine glands throughout the body, such as the pituitary and thyroid gland, and can act on target cells via the blood. Importantly, hormones contribute to homeostasis given their involvement in regulating various functions, such as digestion and absorption, circulation, respiration, immunity, and metabolism, thus maintaining health [1].

Inhibin B is a glycoprotein hormone primarily secreted from Sertoli cells of the testis and ovarian granulosa cells and is a heterodimer composed of α and β subunits cross-linked by disulfide bonds [2]. Gonadotropin-releasing hormone (GnRH) is secreted from the hypothalamus and promotes the secretion of follicle-stimulating hormone (FSH) by acting on the anterior lobe of the pituitary gland [3, 4]. In males, FSH acts on Sertoli cells of the testis to promote spermatogenesis, whereas it acts on ovarian granulosa cells to promote follicle maturation in females. In contrast, inhibin B negatively acts on the hypothalamic-pituitary system and regulates spermatogenesis and follicle maturation by suppressing FSH production [2, 5]. It has been reported that the blood inhibin B concentration can be inversely correlated with FSH levels [6]. Given GnRH secretion from the hypothalamus and reduced Leydig cell responsiveness to FSH and luteinizing hormone, the total serum testosterone concentration in males decreases by 1–2% annually

from approximately 30 years of age [7]. FSH levels tend to increase with age because of decreased testosterone levels. Therefore, inhibin B, which suppresses FSH production, tends to decrease with age.

As hormone levels are hereditary, a genetic factor could be implicated [8]. To date, genome-wide association studies (GWAS) have reported loci associated with sex hormone levels in various populations [9-11]. Recently, we have identified a novel locus 12q21.31 associated with plasma inhibin B levels by GWAS [12]. The leucine-rich repeat and IQ motif containing 1 (*LRR1Q1*) gene is located in this locus. *LRR1Q1*, a gene encoding a protein with a leucine-rich repeat (LRR) and an IQ domain, was highly conserved during evolution (Supplementary Figure S1). LRR is a protein structural motif in which repeating sequences with β -sheet-turn- α -helix structures are arranged in a horseshoe-like manner, and amino acids with 20-30 residues, mainly hydrophobic leucine, can be observed in the repeating sequences. LRR acts on protein-protein interactions and is found in several non-functionally related proteins. The IQ domain is a motif composed of approximately 25 amino acid residues and is widely distributed in nature. This motif binds to calmodulin in a Ca^{2+} -independent manner via an amphipathic 7-turn α -helix structure. Proteins with IQ domains include myosin, electroactive channels, phosphatases, and sperm surface proteins.

LRRIQ1 is most strongly expressed in the testes of humans and is localized to cells in fine ducts and Leydig cells according to the Human Protein Atlas (<http://www.proteinatlas.org>). Inhibin B is also secreted by Sertoli cells of the testis. Therefore, LRRIQ1 is speculated to be significantly involved in regulating inhibin B expression. Inhibin B is known to regulate spermatogenesis by suppressing FSH production, suggesting that LRRIQ1 may contribute to fertility. In the present study, we generated *Lrriq1*^{-/-} mice and determined the effect of *LRRIQ1* on inhibin B production and fertility.

Materials and Methods

Animals

All animal care and experiments were conducted in accordance with the guidelines for animal experiments of Tokushima University and were approved by the ethics committee of Tokushima University (Approval number: T2019-107). C57BL/6N mice were purchased from Clea Japan (Tokyo, Japan). All mice were housed in an air-conditioned room at 23±2°C with 50±10% humidity under controlled lighting conditions (12 h light: 12 h darkness cycle).

*Establishment of *Lrriq1* knockout mice*

Lrriq1 knockout fertilized eggs were established using CRISPR-Cas9 technology by Seturo Tech Co., Ltd (Tokushima, Japan) [13]. To generate *Lrriq1* knockout (*Lrriq1*^{-/-}) mice, Cas9 protein and guide RNA (crRNA: 5'-AGAAGAAATCGAAGCTGAAT-3' and tracrRNA) (Figure 2A) were introduced into C57BL/6N fertilized eggs by electroporation. Cultured embryos were transplanted into the oviducts of foster parent mice to give birth. DNA was extracted from the tail of the mice using NucleoSpin DNA RapidLyse (Takara Bio. Shiga, Japan) and amplified by PCR using specific primers: forward (5'-TGCTAGCCTAAAATGGTGCC-3') and reverse (5'-AGGCCACACACCTGAGAGTA-

3'). The PCR amplicons were cloned into the pMD20 vector (Takara Bio) and sequenced. Sequencing was performed by Eurofins Genomics, Inc (Tokyo, Japan). *Lrrriq1*^{-/-} mice were generated by repeated mating.

RT-PCR and quantitative real-time PCR

Collected mouse tissues were stored at 4°C in RNA solution (Ambion, Austin, TX, USA) until use. Total RNA was isolated from mouse tissues using the RNeasy Mini Kit (Qiagen, Hilden, Germany), and cDNA was synthesized using PrimeScript RT Master Mix (Takara Bio). PCR was performed in a DNA thermal cycler under the following thermal cycling profile: initial denaturation at 94°C for 3 min, followed by 25 cycles of amplification (denaturation at 94°C for 30 s, annealing at 60°C or 57°C for 30 s, and extension at 72°C for 1 min). Real-time PCR was performed using TB Green Premix Ex TaqII (Takara Bio) in the AB 7500 real-time PCR system (Applied Biosystems) according to the following thermal cycling profile: initial denaturation at 95°C for 30 s, followed by 40 cycles of amplification (denaturation at 95°C for 5 s, annealing at 60°C for 10 s, and extension at 72°C for 34 s). Data were analyzed using standard curve methods. The primer sets used are listed in Supplementary Table S1.

Immunoblotting

To analyze the expression of *Lrriq1*, the mouse testes were homogenized in five volumes of lysis buffer (50 mM HEPES-KOH of pH 7.8, 10 mM KCl, 0.1 mM EDTA, 0.1% NP-40, 1 mM DTT, and 1 mM PMSF) and incubated on ice for 10 min. The homogenates were centrifuged at 1,500 g for 10 min at 4 °C, and the supernatants were collected. To analyze the expression of *Inha* and *Inhbb*, mouse testicular tissue extracts were obtained using RIPA Lysis Buffer (Santa Cruz Biotechnology, Heidelberg, Germany) according to the manufacturer's instructions. Protein concentrations were determined using the TaKaRa BCA Protein Assay Kit (Takara Bio). Proteins were separated by sodium dodecyl sulfate-polyacrylamide gel electrophoresis (SDS-PAGE; 10%) and electrotransferred onto a polyvinylidene fluoride membrane (Hybond-P; GE Healthcare Bio-Sciences, Buckinghamshire, England). The membrane was blocked with TBS-T buffer (20 mM Tris-HCl, pH 7.6, 137 mM NaCl, and 0.1% Tween-20) with 5% Block Ace (DS Pharma Biomedical Co. Ltd, Osaka, Japan), and then incubated with primary antibodies at 4°C overnight. After washing in TBS-T buffer, the membrane was incubated with secondary antibodies for 1 h at room temperature. After washing, the proteins were visualized using ECL Plus Western blotting Detection System (GE Healthcare Bio-Sciences), and signals were detected using a luminescent image analyzer LAS-4000 (Fujifilm Corp., Tokyo,

Japan). The following antibodies were used: anti-Actb (1:1,000; Proteintech, Tokyo, Japan, #60008-1-1G), anti-Inha (1:500; Abcam, AP19340A-EV), anti-Inhbb (1:500; CUSABIO, #CSB-PA932977), goat anti-mouse IgG HRP conjugate (1:10,000; Proteintech, #SA00001-1), and goat anti-rabbit IgG HRP conjugate (1:10,000; Proteintech, #SA00001-2). *Lrriq1* polyclonal antibody was generated in rabbits by injecting a synthetic peptide of mouse *Lrriq1* in them (peptides 72–90; 1:500) (Sigma-Aldrich Japan). Densitometry of the visualized bands was quantified using ImageJ (National Institutes of Health, Bethesda, MD, USA).

Fertility test

Mating was performed by allowing one male mouse and two female mice (both seven-week-old) to be housed together in the same cage. Five *Lrriq1*^{-/-} male and ten *Lrriq1*^{-/-} female mice were mated with ten wild-type (WT) females and five WT male mice, respectively. Five WT male mice and ten female mice were mated as a control.

Sperm parameters

The left and right cauda epididymis were harvested from 3-month-old mice, chopped several times with 1 mL of phosphate-buffered saline (PBS) solution, and incubated at

37°C for 15 min. After incubation, 200 µL of sperm suspension was diluted 5-fold with 800 µL of PBS and incubated at 60°C for 1 min. Sperm numbers were counted using a hemocytometer under a light microscope. To measure sperm motility, the chopped cauda epididymis was incubated with 1 mL of PBS solution at 37°C for 15 min, and then 10 µL of sperm suspension was placed on a glass slide and covered with a 24 × 24 cover glass. The numbers of motile and immobile sperm were counted under a light microscope. Sperm motility was calculated from the ratio of the motile sperm count to the total sperm count.

Histology of testicular, epididymal tissues and sperm

Testes and cauda epididymis of 3-month-old mice were fixed in Bouin's solution overnight at room temperature, embedded in paraffin, sectioned at 3-5 µm thickness, deparaffinized, and stained with hematoxylin and eosin (H&E). Spermatozoa collected from the cauda epididymis were spread onto poly L-lysine coated glass slides, air-dried, and fixed by incubation with 4% paraformaldehyde phosphate buffer. The TUNEL assay was performed using an *in situ* Apoptosis Detection Kit (Takara Bio), according to the manufacturer's instructions. The samples were examined using an inverted fluorescence microscope (BIOREVO, KEYENCE. Osaka, Japan).

RNA sequencing and data analyses

RNA from the testes of WT and *Lrrigl*^{-/-} male mice (n=3 each), aged 3 months, was extracted using the RNeasy Mini Kit (QIAGEN). Sequencing libraries were constructed using the TruSeq stranded mRNA library (Illumina, San Diego, CA, USA). RNA sequencing was performed using 100-bp paired-end sequencing on a NovaSeq6000 platform (Illumina). Sequencing experiments were performed by Macrogen, Inc. Raw data obtained by the sequence were quality checked using FastQC [14], and the adapter sequence, low-quality reads, and poor-quality bases were removed using Trimmomatic 0.39 [15]. Subsequently, the cleaned reads were mapped to the mouse reference genome (GRCm38) using the alignment tool STAR [16] to create the BAM format mapping data. After calculating the expression level of each gene unit using RSEM software [17], summarizing the expression level data of all samples and identifying differentially expressed genes (DEGs) between three WT mice and three *Lrrigl*^{-/-} mice were performed using the edgeR package using TCC-GUI [18]. Gene Ontology (GO) biological process enrichment analysis was performed using the Metascape database (<https://metascape.org/>) for DEG with an expression ratio of more than two-fold at $p < 0.05$ [19]. Ingenuity Pathway Analysis (IPA) software (QIAGEN) was used to extract the

canonical pathway with low p -values [20].

Results

*Expressions of *Lrriq1* and *Inhibin B* mRNA in mouse tissues*

The mRNA expression levels of *Lrriq1* and *Inhibin B* in tissues derived from male and female mice were examined by RT-PCR. Inhibin B is a heterodimer consisting of α and β subunits, each encoded by inhibin alpha (*Inha*) and inhibin beta-B (*Inhbb*); therefore, we examined the expression of these genes. *Lrriq1* was specifically expressed in the testes of male mice and was not expressed in any tissue of female mice (Figure 1A). *Inha* showed testis-specific and ovary-specific expression in male and female mice, respectively. *Inhbb* is expressed in several tissues, including the testis, uterus, and ovaries. As *Lrriq1*, *Inha*, and *Inhbb* were expressed in the testis, we confirmed the expression of these genes in male tissues. We observed that *Lrriq1* and *Inhbb* were expressed in the testis, as well as the cauda epididymis and sperm (Figure 1B). *Inha* was weakly expressed in the cauda epididymis but not in sperm. Next, to examine *Lrriq1* temporal expression, *Lrriq1* expression levels were examined in the testes of mice at different postnatal days. *Lrriq1* expression began on day 20 after birth, peaked on day 30, and then maintained stable expression levels (Figure 1C).

*Establishment of *Lrriq1* knockout mice and inhibin B production*

Next, to investigate the effect of *Lrriq1* on inhibin B expression, we generated *Lrriq1* knockout mice. *Lrriq1* knockout mice were established using the CRISPR-Cas9 technology. In total, five male and two female mice were born from 100 *Lrriq1* genome-edited fertilized eggs; among these, the mutation was confirmed in four male mice and one female mouse. To confirm the mutation, cloning was performed on the T-vector, and Sanger sequencing was performed. We obtained mice exhibiting a mutation in which amino acid 21 of *Lrriq1* was substituted, from lysine to a stop codon, by inserting one base (G) (Figure 2A). Mice with this heterozygous mutation were repeatedly mated to establish knockout mice (*Lrriq1*^{-/-} mice). To confirm the successful establishment of *Lrriq1*^{-/-} mice, Sanger sequencing (Figure 2B), western blotting (Figure 2C), RT-PCR (Figure 2D), and real-time PCR (Figure 2E) using cDNA were performed. Sanger sequencing of testis-derived cDNAs of *Lrriq1*^{-/-} mice revealed a G insertion mutation. Western blotting results revealed the presence of *Lrriq1* in WT mice but not in *Lrriq1*^{-/-} mice. Compared with WT mice, *Lrriq1* mRNA expression levels were downregulated in *Lrriq1*^{-/-} mice. This could be due to, probably because the single nucleotide insertion that made mRNA unstable. *Lrriq1*^{-/-} mice were used in the subsequent experiments.

To determine the effect of *Lrriq1* knockout on inhibin B production, the expression of *Inha* and *Inhbb* was examined in WT and *Lrriq1*^{-/-} mice using western

blotting. Compared with WT mice, Inha expression was significantly reduced in the testis of *Lrriq1*^{-/-} mice (Figure 3). Inhbb expression was not detected (data not shown), probably because of its lower expression level. Our findings suggested that Lrriq1 could be involved in regulating the α subunit of inhibin B, which is specifically expressed in the testis.

Effect of Lrriq1 on fertility

Lrriq1 is specifically expressed in the testis, and inhibin B is secreted by Sertoli cells to regulate spermatogenesis, suggesting that LRRIQ1 may contribute to fertility. Accordingly, we examined the effects of Lrriq1 on fertility in WT and *Lrriq1*^{-/-} mice. First, a mating experiment was performed to confirm the fertility of *Lrriq1*^{-/-} male and female mice. The average litter size numbers (with standard deviation [SD]) of WT, *Lrriq1*^{-/-} male, and *Lrriq1*^{-/-} female mice were 8.3 ± 1.3 , 4.3 ± 2.9 and 8.2 ± 2.6 , respectively. The litter size of *Lrriq1*^{-/-} male mice was significantly reduced when compared with that of WT male mice ($p < 0.001$); however, no difference was observed between *Lrriq1*^{-/-} and WT female mice (Figure 4A). Next, we examined sperm number and motility to determine the potential cause underlying the decreased litter size in *Lrriq1*^{-/-} male mice. No difference in sperm number was noted between WT and *Lrriq1*^{-/-} male mice (Figure

4B). The sperm motility (%) of WT and *Lrriq1*^{-/-} male mice was 70.2 ± 4.7 and 48.4 ± 4.9, respectively, and the sperm motility of *Lrriq1*^{-/-} male mice was significantly lower than that of WT male mice ($p < 0.001$) (Figure 4C). These findings suggested that *Lrriq1*^{-/-} male mice exhibited reduced litter size due to decreased sperm motility.

Next, to clarify the underlying cause for reduced sperm motility in *Lrriq1*^{-/-} male mice, testis size and weight were measured, and morphology was examined. However, there were no differences in testis size (Figure 5A, B) and weight (Figure 5C), as well as in the morphology of the testis (Figure 5D), cauda epididymis (Figure 5E), and sperm (Figure 5F).

RNA sequence analysis of WT and Lrriq1^{-/-} mouse testis

To determine the mechanism through which *Lrriq1* affects sperm motility, we examined gene expression in WT and *Lrriq1*^{-/-} mice by RNA-Seq analysis. On performing expression fluctuation analysis in WT and *Lrriq1*^{-/-} mice, 10435 genes were detected as significant DEGs (false discovery rate [FDR] < 0.1) (Figure 6A). The top 30 DEGs are shown in a heat map (Figure 6B) and Supplementary Table S2, and several of these genes are known to be involved in spermatogenesis and meiosis. The highest DEG was gene 14569 (*Gm14569*), which is an ortholog of the human acrosomal protein KIAA1210,

followed by HORMA domain containing 1 (*Hormad1*) and synaptonemal complex protein 3 (*Sycp3*). Compared with WT mice, expression levels of these genes were decreased in *Lrriq1*^{-/-} mice. *Lrriq1*, *Inha*, and *Inhbb* were also detected as DEGs, and their expression levels were decreased in *Lrriq1*^{-/-} mice when compared with WT mice (Supplementary Figure S2). Next, enrichment analysis was performed using the Metascape database to investigate the functions of several genes in the DEGs. We noted that many genes involved in the meiotic cell cycle were present among the DEGs (Figure 6C). In addition, as a result of canonical pathway analysis using IPA, many genes involved in the sperm motility signal transduction pathway were listed among the DEGs, and it was predicted that the activation of this pathway is suppressed based on the available literature (Figure 6D). Molecules involved in the sperm motility pathway are listed in Supplementary Figure S3.

Detection of apoptosis in the reproductive organs

Given that knockdown of *INHA* [21] and *INHBB* [22] subunits of inhibin B can induce apoptosis, a TUNEL assay was performed to examine apoptosis in the testis and cauda epididymis of WT and *Lrriq1*^{-/-} mice. Almost no apoptosis-positive cells were detected in the testes of WT mice, whereas numerous apoptosis-positive cells were found in *Lrriq1*^{-/-}

^{-/-} mice (Figure 7). In addition, several apoptotic sperm were detected in the cauda epididymis of *Lrriq1*^{-/-} mice. Accordingly, our findings indicated that the knockout of *Lrriq1* induces testicular germ cells and epididymal spermatozoa.

Discussion

In the present study, we examined the effect of *Lrriq1*, which is associated with male plasma inhibin B levels by GWAS, on inhibin B production and fertility. First, WT mice were used to analyze the expression of *Lrriq1* gene in several tissues. Accordingly, we observed the testis-specific expression of *Lrriq1*. Furthermore, *Lrriq1* was expressed in the cauda epididymis and sperm. Sperm produced in the testis acquire motility and fertility while moving through the epididymis through the efferent ducts. Therefore, it is possible that *Lrriq1* on the epididymis affects sperm maturation or that *Lrriq1* directly contributes to sperm motility. In addition, on analyzing the time course of *Lrriq1* expression, we noted that *Lrriq1* expression was initiated at approximately day 20 postnatally and then increased with increasing age. In mice, meiosis is initiated at approximately postnatal day 10, and haploid sperm are produced by postnatal day 20, followed by activation of sexual maturation [23]. Therefore, *Lrriq1* may play a role in spermatogenesis.

Lrriq1^{-/-} mice were generated and analyzed for the testicular expression of *Inha* and *Inhbb*. *Inha* expression decreased at both mRNA and protein levels in *Lrriq1*^{-/-} mice. Considering that both *Lrriq1* and *Inha* were expressed in a testis-specific manner in males, *Lrriq1* may be involved in regulating *Inha* expression among inhibin B subunits. LRRIQ1

is known to interact with proteins such as activin A receptor type 1 (ACVR1), activating A receptor type 2A (ACVR2A), and activating A receptor type 2 B (ACVR2B) [24]. Activin, in contrast to inhibin, promotes the secretion of FSH. Therefore, following knockout, *Lrriq1* could not interact with the activin receptor and may have lost the function on the activin receptor. This may have suppressed the synthesis and secretion of FSH, and in turn, suppressed inhibin expression via negative feedback. In the future, it is necessary to clarify the mechanism through which *Lrriq1* is involved in the expression of *Inha*.

We examined the fertility of *Lrriq1*^{-/-} male and *Lrriq1*^{-/-} female mice by mating experiments and noted that *Lrriq1*^{-/-} male mice had a significantly smaller litter size than WT mice. Additionally, examining sperm motility in WT and *Lrriq1*^{-/-} mice confirmed that sperm motility was significantly reduced in *Lrriq1*^{-/-} mice when compared with WT mice. Sperm motility can significantly impact fertility. These results suggest that knockout of the *Lrriq1* gene reduced sperm motility in male mice, subsequently decreasing the fertilization rate and resulting in smaller litter sizes. Next, to investigate the cause of decreased sperm motility in *Lrriq1*^{-/-} male mice, we examined the effects of *Lrriq1* gene knockout on reproductive organs and sperm morphology; however, no morphological differences were observed. Therefore, to analyze the effect of *Lrriq1*,

RNA-Seq analysis was performed. As a result, *Gm14569*, *Hormad1*, and *Sycp3* were ranked as top DEGs. *Gm14569* is a mouse ortholog of human KIAA1210, and KIAA1210 is known to be mainly expressed in the testis. In particular, it is localized near the XY body of spermatocytes, the acrosome of sperm, and ectoplasmic specialization, which is an intercellular adhesion device in Sertoli cells. KIAA1210 has a topoisomerase 2 (*TOP2*)-related protein PAT1 domain, and it has been suggested that it may interact with TOP2 and participate in dynamic changes in the chromatin structure during spermatogenesis [25]. *Hormad1* is a gene localized in the testis and is essential for meiosis during spermatogenesis. Single nucleotide polymorphisms in *HORMAD1* have been associated with human azoospermia caused by meiosis [26]. *Sycp3* encodes an essential component of the synaptonemal complex involved in meiotic synapsis, recombination, and separation. Homozygous null mutations in *Sycp3* cause azoospermia with meiotic arrest in mice [27]. Thus, several genes involved in spermatogenesis and meiosis were found in the top DEGs. In addition, enrichment analysis revealed that the meiotic cell cycle was the most enriched, and canonical pathway analysis revealed that genes involved in the sperm motility signaling pathway were downregulated in *Lrriq1*^{-/-} mice. Accordingly, the results of this analysis support a reduction in sperm motility in *Lrriq1*^{-/-} mice.

Apoptosis in the testis and cauda epididymis of WT and *Lrriq1*^{-/-} mice was

examined using the TUNEL assay. As a result, higher levels of apoptosis were detected in testicular germ cells and epididymal sperm of *Lrriq1*^{-/-} mice than in WT mice. As mentioned earlier, sperm produced in the testis acquire motility and fertility while moving through the epididymis via the efferent ducts. It is estimated that 75% of sperm undergo cell death due to apoptosis during spermatogenesis, and it is considered that apoptosis due to stress is strongly associated with sperm quality [23]. Therefore, it was suggested that induction of epididymal sperm apoptosis reduced sperm motility and decreased litter size in *Lrriq1*^{-/-} male mice. Furthermore, as *Lrriq1* was also expressed in sperm, *Lrriq1* expressed on epididymal sperm may be involved in suppressing apoptosis via an unknown mechanism. Apoptosis was observed in majority of testicular Leydig cells. Leydig cells secrete testosterone, which acts on Sertoli cells in maintaining spermatocyte and testicular functions [28]. Therefore, apoptosis of Leydig cells negatively affects spermatogenesis and testicular function. However, our results showed that apoptosis in Leydig cells did not differ between WT and *Lrriq1*^{-/-} mice. Therefore, it is unlikely that *Lrriq1*^{-/-} mice have reduced sperm motility due to apoptosis in Leydig cells.

In conclusion, our findings indicate that the knockout of *Lrriq1* reduced sperm motility and litter size by inducing apoptosis of testicular germ cells and epididymal sperm. *Lrriq1* plays an important role in regulating the expression of inhibin B and is an

essential factor for fertility by suppressing apoptosis.

References

[1] Kang J, Scholp A, Jiang JJ. A Review of the Physiological Effects and Mechanisms of Singing. *J Voice*. 2018;32(4):390–5. doi:10.1016/j.jvoice.2017.07.008.

[2] Zou G, Ren B, Liu Y, Fu, Y, Chen P, Li X, et al. Inhibin B suppresses anoikis resistance and migration through the transforming growth factor- β signaling pathway in nasopharyngeal carcinoma. *Cancer Sci*. 2018;109(11): 3416–27. doi: 10.1111/cas.13780.

[3] Belchetz PE, Plant TM, Nakai EJ, Knobil E. Hypophysial responses to continuous and intermittent delivery of hypothalamic gonadotropin-releasing hormone. *Science*. 1978;202(4368): 631–3. doi: 10.1126/science.100883.

[4] Smith, M.A., and Vale, W.W. (1981) Desensitization to gonadotropin-releasing hormone observed in superfused pituitary cells on Cytodex beads. *Endocrinology*.

1981;108(3): 752–9. doi: 10.1210/endo-108-3-752.

[5] Meachem SJ, Nieschlag E, Simoni M. Inhibin B in male reproduction: pathophysiology and clinical relevance. *Eur J Endocrinol.* 2001;145(5): 561–71. doi: 10.1530/eje.0.1450561.

[6] Guerra-Garcia. R, Franc. J, Gonzales GF. Serum inhibin is inversely correlated with serum FSH levels in adult men. *Arch Androl.* 1989;22(1): 35–40. doi: 10.3109/01485018908986748.

[7] Elmlinger MW, Dengler T, Weinstock C, Kuehnel W. Endocrine alterations in the aging male. *Clin Chem Lab Med.* 2003;41(7):934–41. doi: 10.1515/CCLM.2003.142.

[8] Kuijper EA, Lambalk CB, Boomsma DI, van der Sluis S, Blankenstein MA, de Geus, et al. Heritability of reproductive hormones in adult male twins. *Hum Reprod.* 2007;22(8):2153–9. doi: 10.1093/humrep/dem145.

[9] Ohlsson C, Wallaschowski H, Lunetta KL, Stolk L, Perry JR, Koster A, et al. 2011

Genetic determinants of serum testosterone concentrations in men. *PLoS Genet.* 2011;7(10): e1002313. doi: 10.1371/journal.pgen.1002313.

[10] Jin G, Sun J, Kim. ST, Feng J, Wang Z, Tao S, et al. Genome-wide association study identifies a new locus JMJD1C at 10q21 that may influence serum androgen levels in men. *Hum Mol Genet.* 2012;21(23):5222–8. doi: 10.1093/hmg/dds361.

[11] Chen Z, Tao S, Gao Y, Zhang J, Hu Y, Mo L, et al. (2013) Genome-wide association study of sex hormones, gonadotropins and sex hormone-binding protein in Chinese men. *J Med Genet.* 2013;50(12):794–801. doi: 10.1136/jmedgenet-2013-101705.

[12] Sato Y, Tajima A, Kiguchi M, Kogusuri S, Fujii A, Sato T, et al. Genome-wide association study of semen volume, sperm concentration, testis size, and plasma inhibin B levels. *J Hum Genet.* 2020;65(8): 683–91. doi: 10.1038/s10038-020-0757-3.

[13] Hashimoto M, Yamashita Y, Takemoto T. Electroporation of Cas9 protein/sgRNA into early pronuclear zygotes generates non-mosaic mutants in the mouse. *Dev Biol.* 2016;418(1):1–9. doi: 10.1016/j.ydbio.2016.07.017.

[14] Andrews S. FASTQC. A quality control tool for high throughput sequence data.2010; <http://www.bioinformatics.babraham.ac.uk/projects/fastqc/>

[15] Bolger AM, Lohse M, Usadel B. Trimmomatic: a flexible trimmer for Illumina sequence data. *Bioinformatics*. 2014;30(15):2114–20. doi: 10.1093/bioinformatics/btu170.

[16] Dobin A, Davis CA, Schlesinger F, Drenkow J, Zaleski C, Jha S, et al. STAR: ultrafast universal RNA-seq aligner. *Bioinformatics*. 2013;29(1):15–21. doi: 10.1093/bioinformatics/bts635.

[17] Li B, Dewey CN. RSEM: accurate transcript quantification from RNA-Seq data with or without a reference genome. *BMC Bioinformatics*. 2011;12:323. doi: 10.1186/1471-2105-12-323.

[18] Su W, Sun J, Shimizu K, Kadota K. TCC-GUI: a Shiny-based application for differential expression analysis of RNA-Seq count data. *BMC Res Notes*. 2019;12(1):133.

doi: 10.1186/s13104-019-4179-2.

[19] Zhou Y, Zhou B, Pache L, Chang M, Khodabakhshi AH, Tanaseichuk O, et al. Metascape provides a biologist-oriented resource for the analysis of systems-level datasets. *Nat Commun.* 2019;10(1):1523. doi: 10.1038/s41467-019-09234-6.

[20] Krämer A, Green J, Pollard J, Jr Tugendreich S. Causal analysis approaches in Ingenuity Pathway Analysis. *Bioinformatics.* 2014;30(4):523–30. doi: 10.1093/bioinformatics/btt703.

[21] Cui Z, Liu L, Zhu Q, Wang Y, Yin H, Li D, et al. Inhibin A regulates follicular development via hormone secretion and granulosa cell behaviors in laying hens. *Cell Tissue Res.* 2020;381(2):337–50. doi: 10.1007/s00441-020-03207-8.

[22] M'baye M, Hua G, Khan HA, Yang L. RNAi-mediated knockdown of INHBB increases apoptosis and inhibits steroidogenesis in mouse granulosa cells. *J Reprod Dev.* 2015;61(5):391–7. doi: 10.1262/jrd.2014-158.

[23] Print CG, Loveland KL. Germ cell suicide: new insights into apoptosis during spermatogenesis. *Bioessays*. 2000;22(5):423–30. doi: 10.1002/(SICI)1521-1878(200005)22:5<423::AID-BIES4>3.0.CO;2-0.

[24] Huttlin EL, Bruckner RJ, Paulo JA, Cannon JR, Ting L, Baltier K, et al. Architecture of the human interactome defines protein communities and disease networks. *Nature*. 2017;545(7655):505–9. doi: 10.1038/nature22366.

[25] Iwamori T, Iwamori N, Matsumoto M, Ono E, Matzuk MM. Identification of KIAA1210 as a novel X-chromosome-linked protein that localizes to the acrosome and associates with the ectoplasmic specialization in testes. *Biol Reprod*. 2017;96(2): 469–77. doi: 10.1095/biolreprod.116.145458.

[26] Miyamoto T, Tsujimura A, Miyagawa Y, Koh E, Namiki M, Horikawa M, et al. Single-nucleotide polymorphisms in *HORMAD1* may be a risk factor for azoospermia caused by meiotic arrest in Japanese patients. *Asian J Androl*. 2012;14(4):580–3. doi: 10.1038/aja.2011.180.

[27] Yuan L, Liu JG, Zhao J, Brundell E, Daneholt B, Höög C. The murine SCP3 gene is required for synaptonemal complex assembly, chromosome synapsis, and male fertility. *Mol Cell*. 2000;5(1):73–83. doi: 10.1016/s1097-2765(00)80404-9.

[28] De Gendt K, Swinnen JV, Saunders PT, Schoonjans L, Dewerchin M, Devos A, et al. A Sertoli cell-selective knockout of the androgen receptor causes spermatogenic arrest in meiosis. *Proc Natl Acad Sci U S A*. 2004;101(5):1327–32. doi: 10.1073/pnas.0308114100.

Figure legends

Figure 1. The mRNA expression of *Lrriq1*, *Inha*, and *Inhbb* by RT-PCR.

(A) The mRNA expression of *Lrriq1*, *Inha*, and *Inhbb* in several tissues from three-month-old male and female mice. (B) The mRNA expression of *Lrriq1*, *Inha*, and *Inhbb* in testis, cauda epididymis, and sperm. (C) Postnatal changes in *Lrriq1* mRNA expression in the male testis. *Actb* was used as a control. M, marker.

Figure 2. Establishment of *Lrriq1* knockout mice.

(A) The entire *Lrriq1* gene, nucleotide, and amino acid sequences of Exon2 are shown.

In the upper panel, bold lines indicate exons of the *Lrriq1* gene. In the middle figure, the blue color indicates crRNA sequences and the orange color indicates PAM sequences. The lower figure shows the genotype sequence of *Lrriq1* knockout mice. The insertion of a single base (G) caused a frameshift in which the amino acid 21 of *Lrriq1* was substituted from lysine to the stop codon. **(B)** Nucleotide sequence of cDNA in WT and *Lrriq1*^{-/-} mouse. **(C)** The expression of *Lrriq1* in 3-month-old WT and *Lrriq1*^{-/-} mouse testes by western blotting. The mRNA expression of *Lrriq1* in WT and *Lrriq1*^{-/-} mice by RT-PCR **(D)** and real-time PCR **(E)**. *Lrriq1* mRNA expression levels were normalized by *Actb*. Data indicates average \pm SD (n=5). Statistically significant differences: ** $p < 0.01$; Student's *t*-test. SD, standard deviation; WT, wild-type.

Figure 3. Protein expression levels of Inha by western blotting

The left panel indicates the expression of *Inha* in 3-month-old WT and *Lrriq1*^{-/-} mouse testes by western blotting. The right panel indicates the quantitative analysis of *Inha* protein expression levels. *Inha* expression levels were normalized to that of *Actb*. Data are presented as the mean \pm SD (n=3). Statistically significant differences: ** $p < 0.01$; Student's *t*-test. SD, standard deviation; WT, wild-type.

Figure 4. Effect of *Lrriq1* on fertility.

(A) The litter size of WT and *Lrriq1*^{-/-} mice. Five *Lrriq1*^{-/-} male and ten *Lrriq1*^{-/-} female mice were mated with ten WT female and five WT male mice (all 7-week-old), respectively. As a control, five WT male mice and ten female mice were mated (7-week-old). The litter size number of ten female mice is presented as the average ± SD. (B) The sperm counts of WT and *Lrriq1*^{-/-} mice. The sperm counts of mice are presented as the average ± SD (n=5). (C) The sperm motility of WT and *Lrriq1*^{-/-} mice. The sperm motility (%) is presented as average ± SD (n=5). Statistically significant differences: **p* < 0.05, ****p* < 0.001; Student's *t*-test. SD, standard deviation; WT, wild-type.

Figure 5. Effect of *Lrriq1* on reproductive organs and sperm.

(A) Testis of 3-month-old WT and *Lrriq1*^{-/-} mice. (B) Testis size of WT and *Lrriq1* mice. Testis size is presented as the average ± SD (n=5). (C) Testis weight of WT and *Lrriq1* mice. Testicular weight is presented as the average ± SD (n=5). (D) H&E staining of testes of 3-month-old WT and *Lrriq1*^{-/-} mice. (E) H&E staining of cauda epididymis of 3-month-old WT and *Lrriq1*^{-/-} mice. (F) Sperm of 3-month-old WT and *Lrriq1* mice. SD, standard deviation. H&E, hematoxylin and eosin; WT, wild-type.

Figure 6. RNA-Seq analysis of testis of 3-month-old WT and *Lrriq1*^{-/-} mice.

(A) MA plot with q value < 0.1 (10% FDR). The vertical axis M shows the difference between the \log_2 converted signal values, and the horizontal axis A shows the average value of \log_2 converted signal values. DEGs are presented as green plots and non-DEGs as black plots. The red arrow indicates *Lrriq1*, *Inha*, and *Inhbb*, and the black arrow indicates the top three genes. (B) Heatmap of the top 30 DEGs. The heatmap shows the top 30 genes with differential expression in the testes of WT and *Lrriq1*^{-/-} mice. The darker the red color, the higher the expression level, and the darker the blue color, the lower the expression level. (C) Metascape bar graph for viewing top 20 enrichment GO terms. The meiotic cell cycle was the most enriched of DEGs. (D) Canonical pathway of the top 20 low p -values using IPA software. Blue colors indicate a negative z -score, and gray colors indicate no activity pattern available. Darker colors indicate high absolute z -scores. The sperm motility pathway was extracted in second place. FDR, false discovery rate; DEG, differentially expressed gene. GO, Gene Ontology. IPA, Ingenuity Pathway Analysis; WT, wild-type.

Figure 7. Detection of apoptosis in the testis and cauda epididymis by TUNEL assay.

TUNEL staining of testis and cauda epididymis sections of 3-month-old WT and *Lrriq1*^{-/-}

^{1/} mice.

Statements and Declarations

Funding

This study was supported in part by Grant-in-Aids for Scientific Research (B) (17H04331) (to Y.S).

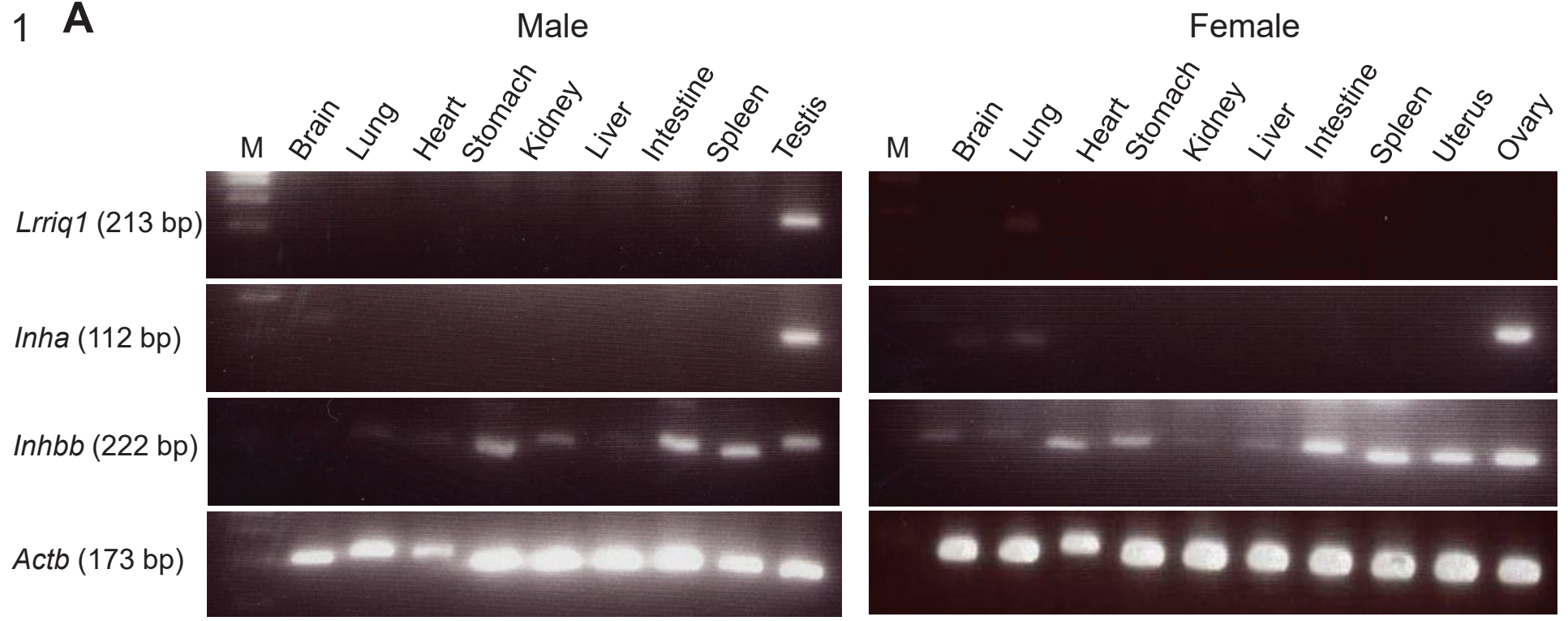
Conflict of Interest

The authors declare no conflict of interest.

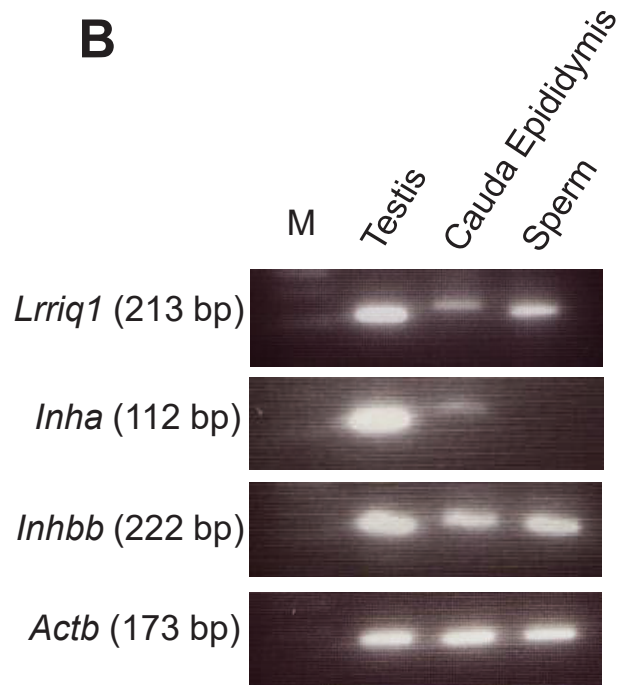
Acknowledgments

This study was supported by the Support Center for Advanced Medical Sciences, Tokushima University Graduate School of Biomedical Sciences. We would like to thank Editage (www.editage.com) for English language editing.

Figure 1 **A**



B



C

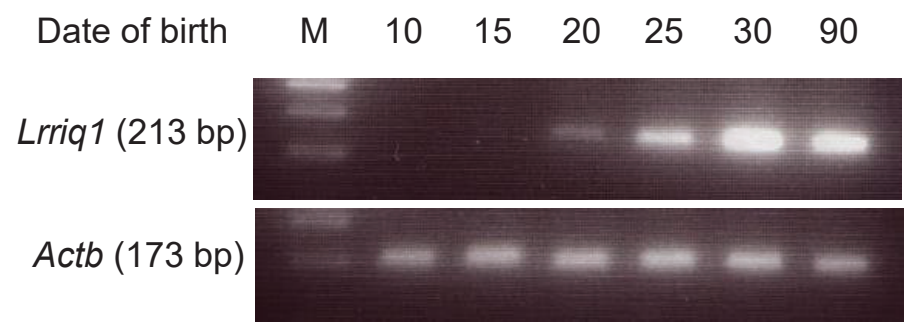


Figure 2

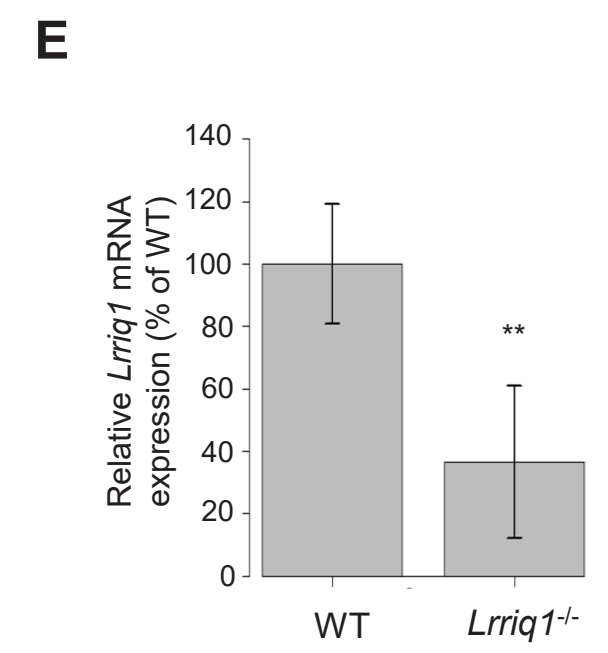
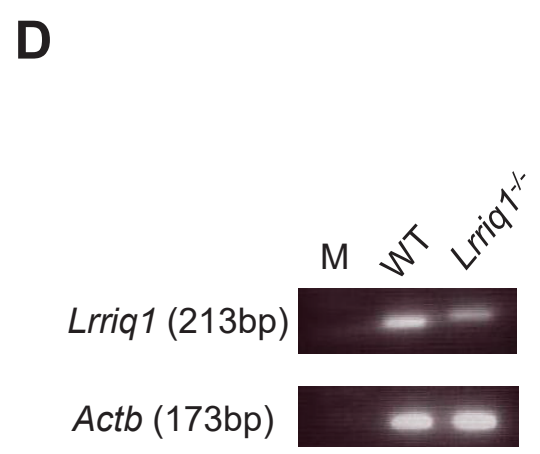
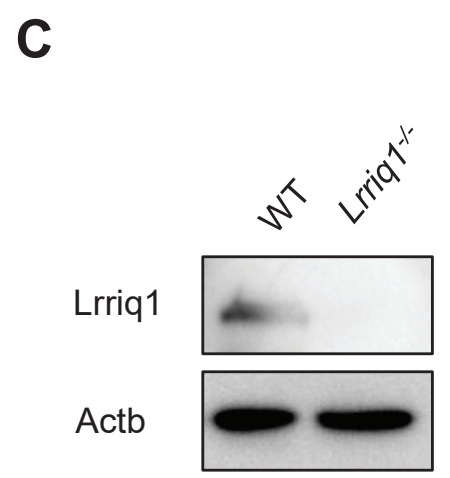
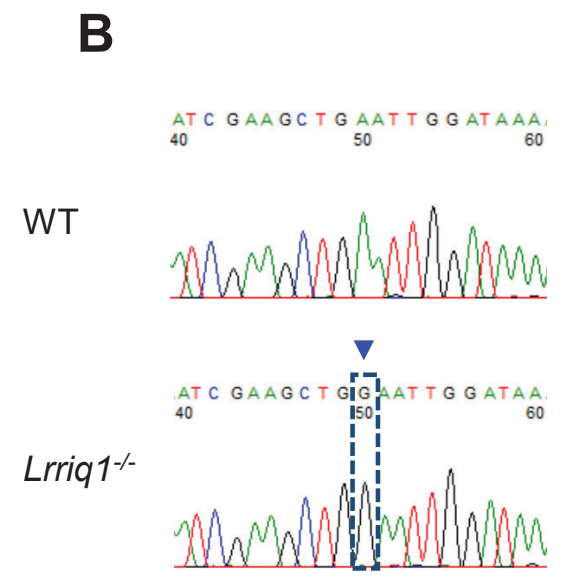
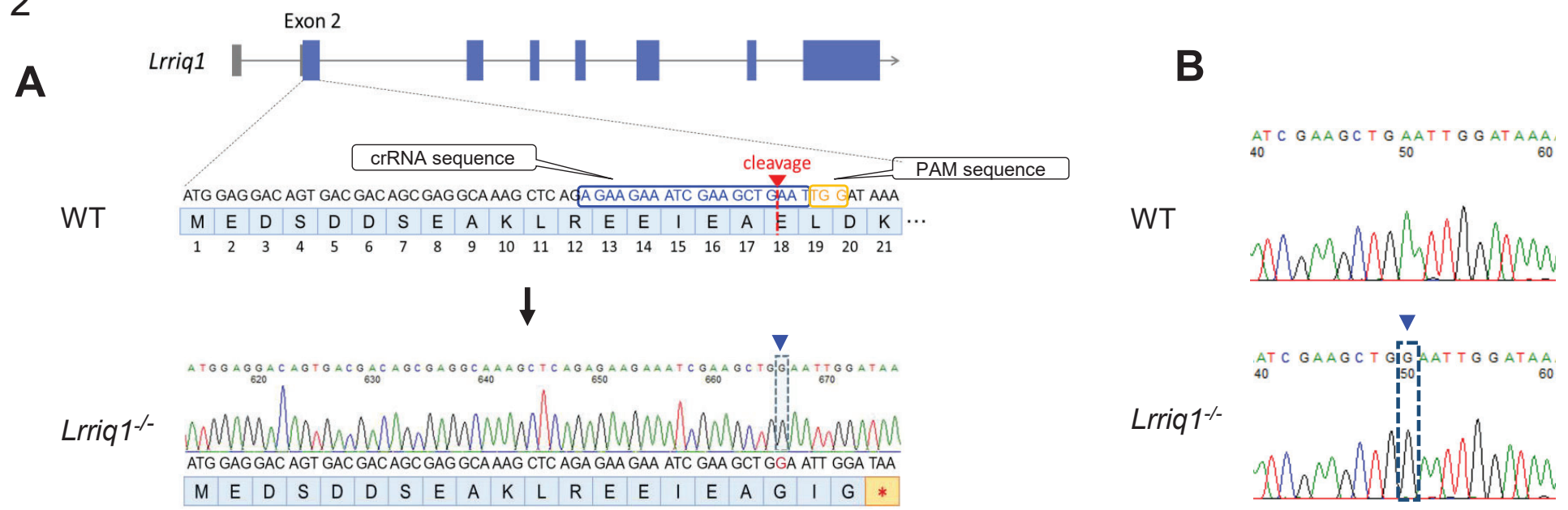


Figure 3

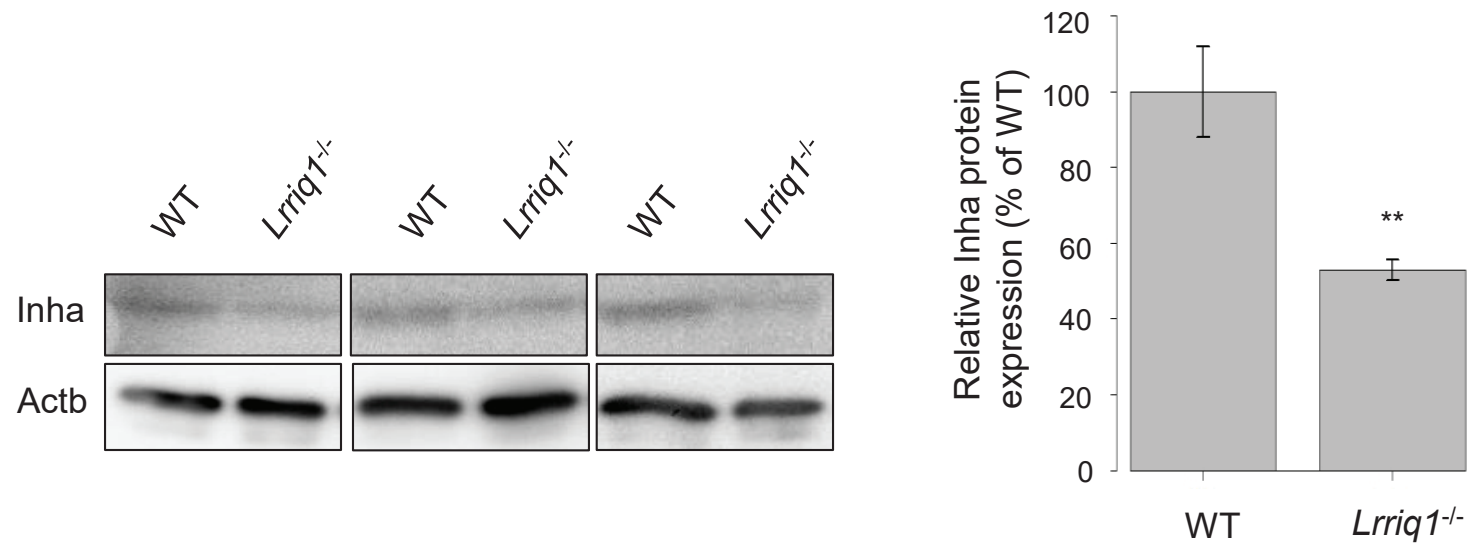
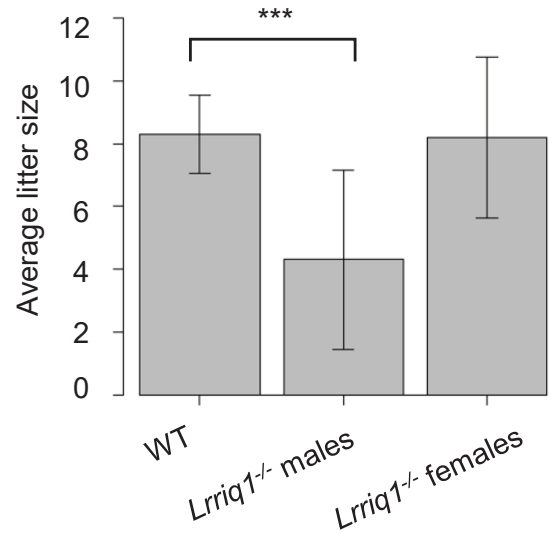
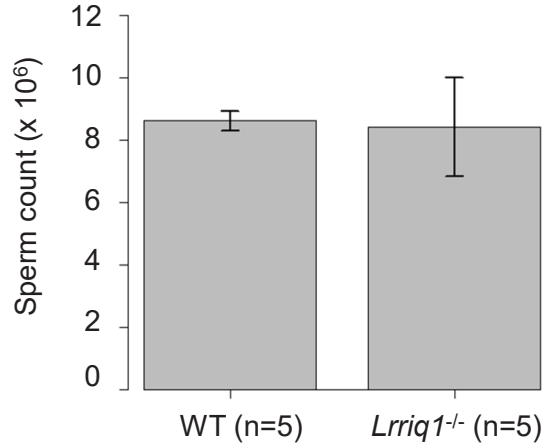


Figure 4

A



B



C

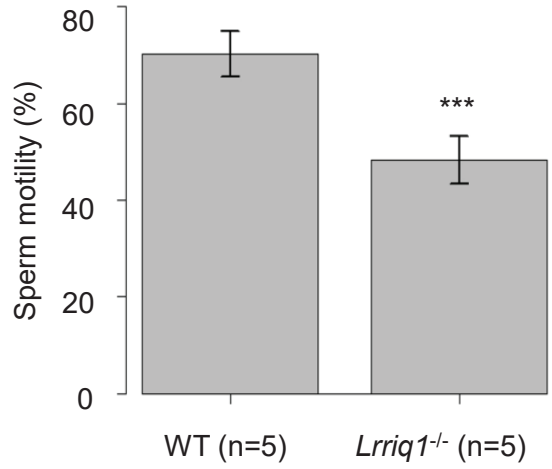


Figure 5

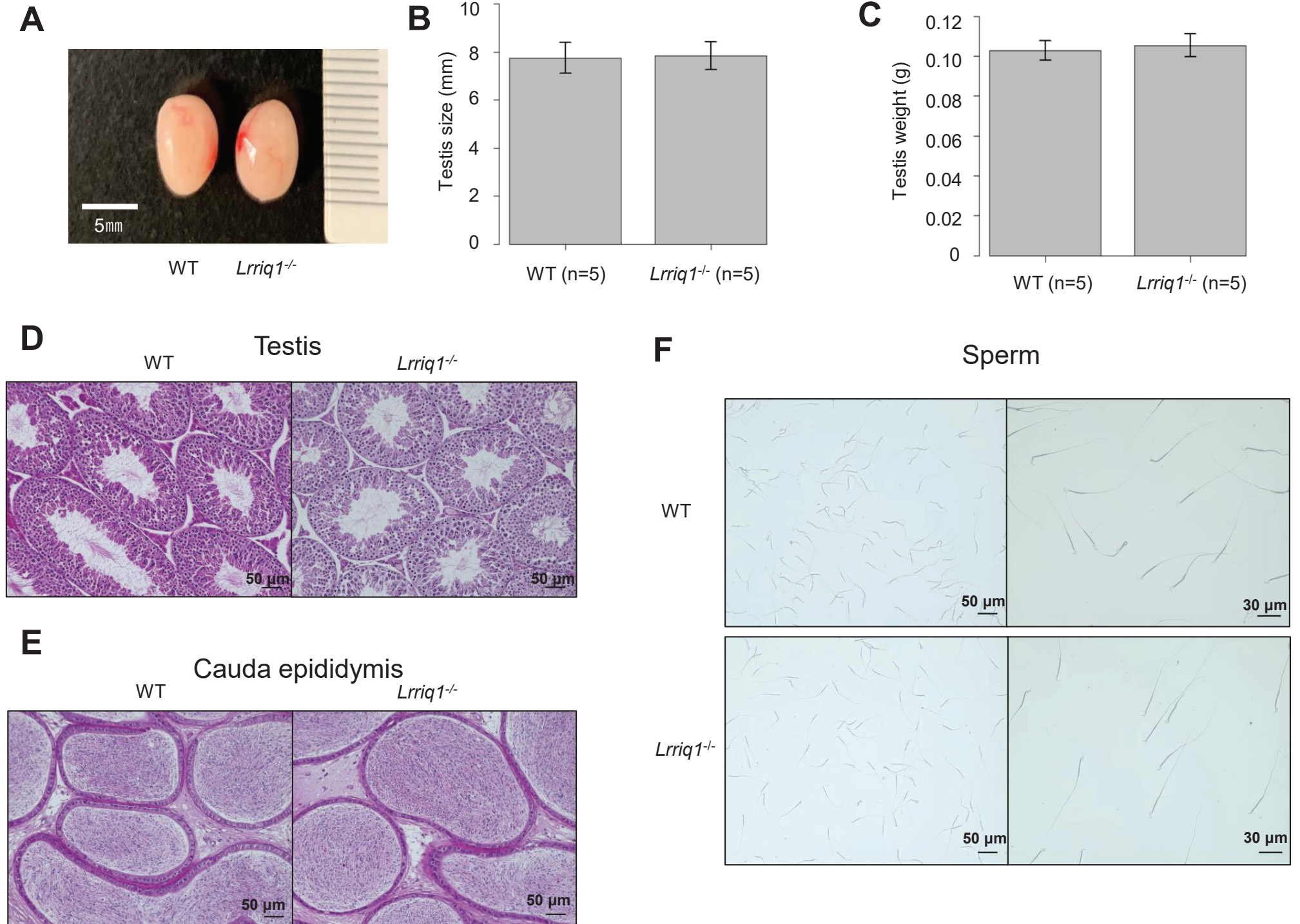


Figure 6

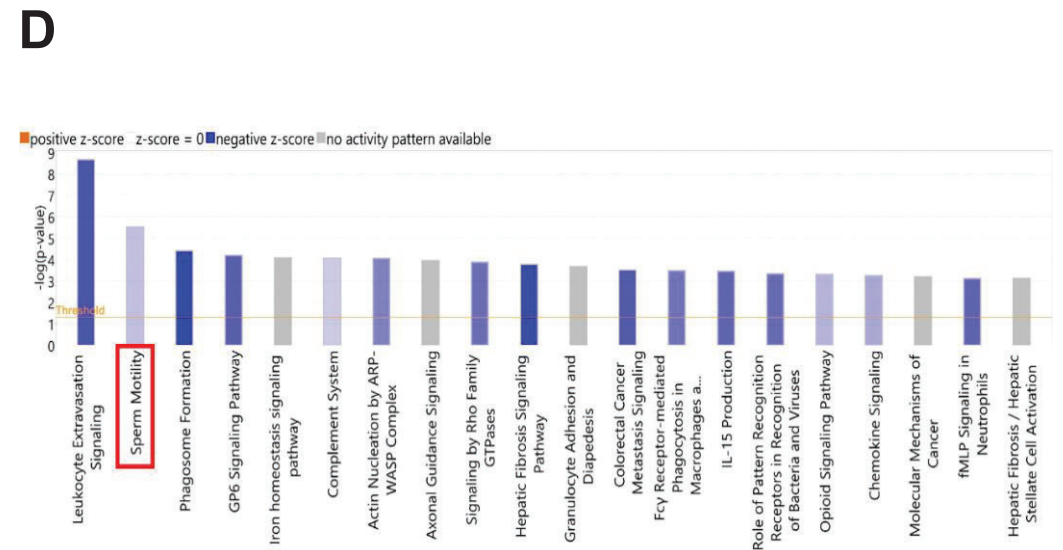
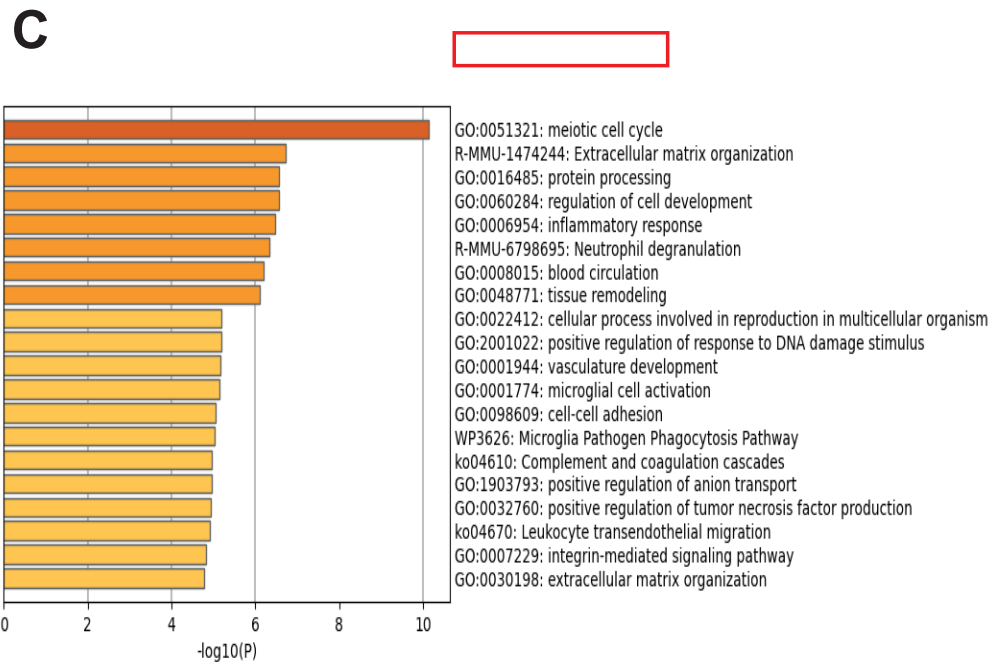
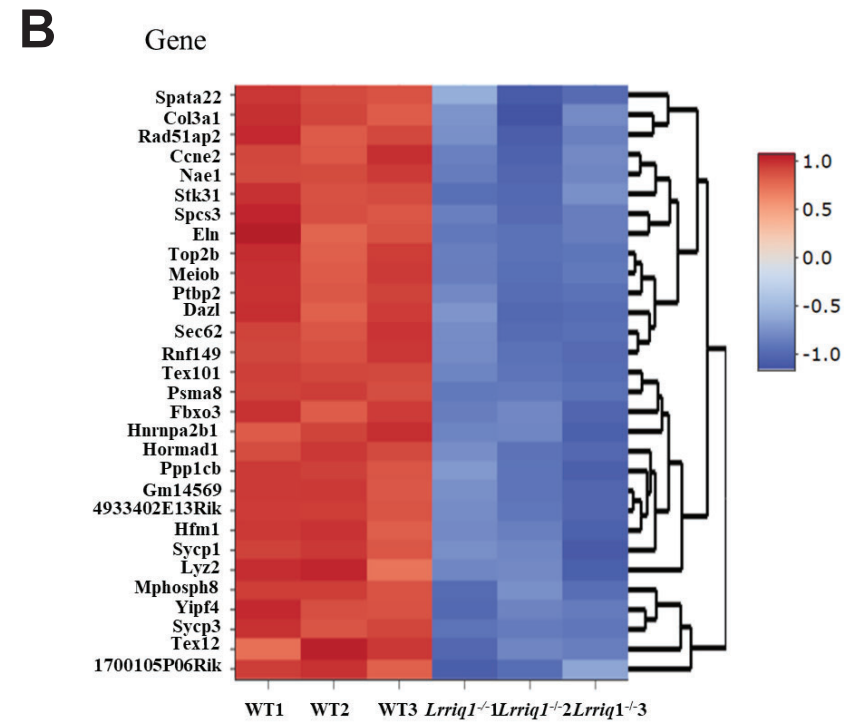
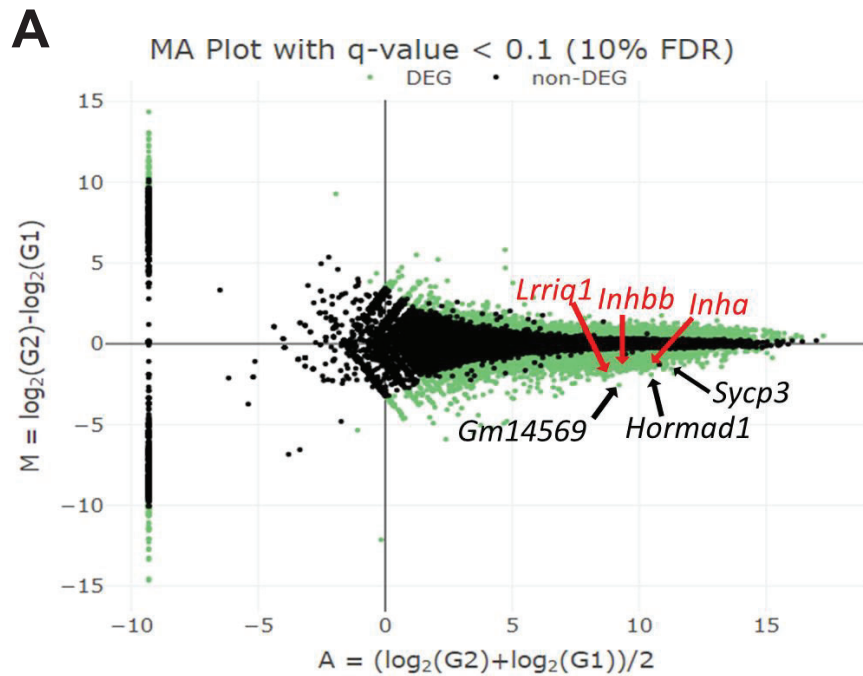
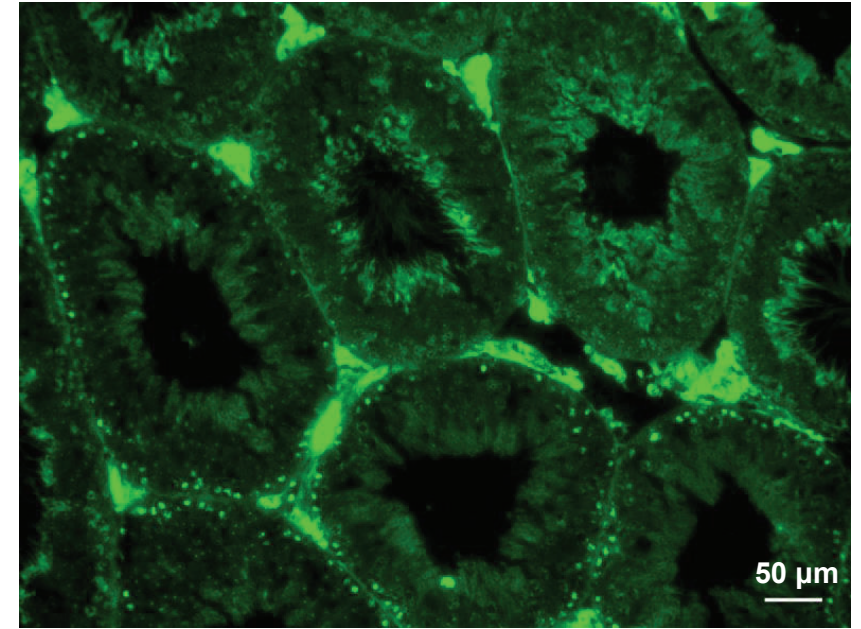
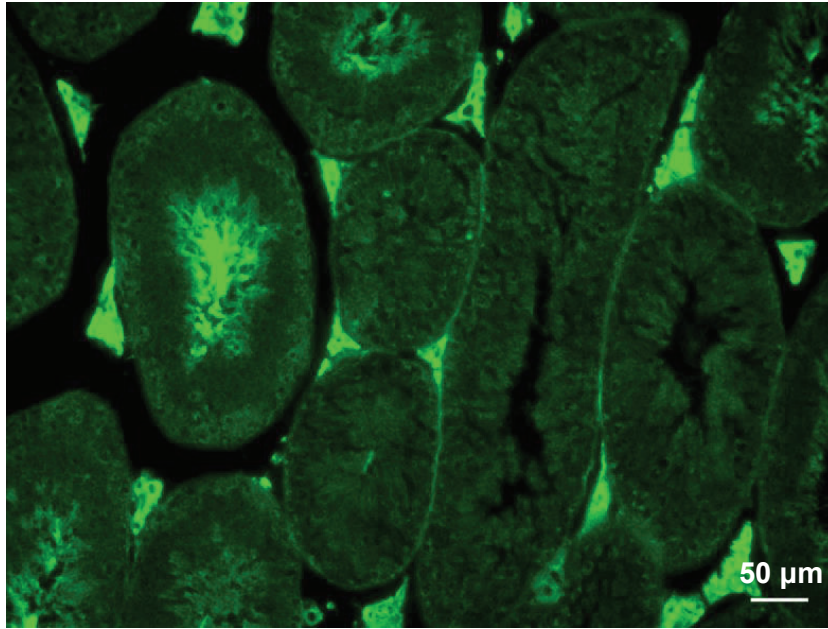


Figure 7

WT

Lrrig1^{-/-}

Testis



Cauda Epididymis

